DOI: 10.1002/ejic.201000669

Back to the Coordination Modes of the Thiosemicarbazonate Chain: New Insights from Diorganolead(IV) and Lead(II) Derivatives of Isatin-3-thiosemicarbazone

José S. Casas,*[a] Noelia Casanova,[a] María S. García-Tasende,[a] Agustín Sánchez,[a] José Sordo,[a] Ángeles Touceda,[a] and Saulo Vázquez[b]

Keywords: Lead / Coordination modes / Thermodynamics

The syntheses and characterizations of the new heteroleptic complexes $[PbPh_2(OAc)(N^2\text{-}L^1)]\cdot MeOH\cdot EtOH$, $[PbPh_2(OAc)(N^3\text{-}L^2)]\cdot H_2O$, $[Pb(OAc)(N^2\text{-}L^1)]$, $[Pb(OAc)(N^3\text{-}L^1)]\cdot 3H_2O$ and $[Pb(OAc)(N^2\text{-}L^2)]$ {HL^1 = isatin-3-thiosemicarbazone, HL^2 = isatin-3-(N^1-methylthiosemicarbazone); $N^2\text{-}L^x$ = thiosemicarbazonate bound through O,S and the hydrazinic [N(2)] nitrogen atom; $N^3\text{-}L^x$ = thiosemicarbazonate bound through the O,S and the iminic [N(3)] nitrogen atom} are described. The single-crystal X-ray structures of HL^2, $[PbPh_2(OAc)(N^2\text{-}L^1)]\cdot MeOH\cdot EtOH$, $[PbPh_2(OAc)(N^3\text{-}L^2)]\cdot H_2O$, $[Pb(OAc)(N^2\text{-}L^1)]$ and $[Pb(OAc)(N^3\text{-}L^1)]\cdot 3H_2O$ have been solved. The organometallic compounds $[PbPh_2(OAc)(N^2\text{-}L^1)]\cdot MeOH\cdot EtOH$ and $[PbPh_2(OAc)(N^3\text{-}L^2)]\cdot H_2O$ have a roughly similar distorted bipyramidal pentagonal stereochemistry, with apical phenyl groups and both the O,N^x,S-coordinated L^{x-} and the anisobidentate AcO^- ligands in the equatorial plane. In $[PbPh_2(OAc)(N^2\text{-}L^1)]\cdot MeOH\cdot EtOH$, the $(N^2\text{-}L^1)^-$ ligand forms a four- and a six-membered chelate ring with the metal, whereas in $PbPh_2(OAc)(N^3\text{-}L^2)]\cdot H_2O$ the two chelate rings formed by $(N^3\text{-}L^2)^-$ are five-membered. The Pb^{II} complexes, $[Pb(OAc)(N^2\text{-}L^1)]$ and $[Pb(OAc)(N^3\text{-}L^1)]$, which were isolated from the same solution, are linkage isomers. These compounds have a rather irregular stereochemistry that suggests the presence of a stereochemically active lone electron pair; in $[Pb(OAc)(N^2\text{-}L^1)]$ the $(L^1)^-$ ligand is O,N^2,S-coordinated and in $[Pb(OAc)(N^3\text{-}L^1)]$ this ligand is O,N^3,S-coordinated. Analyses of all these systems in solution by ^1H and ^{13}C NMR spectroscopy showed that during synthesis the kinetically controlled O,N^2,S isomer formed first due to the rigidity of the ligand. If the compound remains in solution, slow partial evolution to the O,N^3,S isomer occurs. DFT calculations predict that $[Pb(OAc)(N^3\text{-}L^1)]$ is slightly more stable than $[Pb(OAc)(N^2\text{-}L^1)]$ both in the gas phase and in DMSO solution. The calculations also modelled structures for the two isomers close to those obtained by X-ray diffraction studies.

Introduction

Although thiosemicarbazones (HTSC, Scheme 1) are weakly acidic molecules ($pK_a \approx 11$–12),[1] in the presence of metal ions they easily lose a proton from the N^3-N^{2}H moiety to generate the thiosemicarbazonate anion, which adopts the tautomeric thiolic form (TSC$^-$, Scheme 1). This form reacts with the metal ion and gives stable complexes that, in the solid state, usually contain the TSC$^-$ ligand bound to the M^{n+} species through the thiolic sulfur and the azamethinic nitrogen (N^3), giving rise to a five-membered chelate ring (**A**, Scheme 2). When R^3 and/or R^4 are hydrogen atoms, the general conformation of HTSC is that shown in Scheme 1. This arrangement allows the formation of an N^3···H–N^1 hydrogen bond, so coordination mode **A** in Scheme 2 involves the spatial rearrangement of the free ligand (with the S atom *trans* to N^3) by rotating the thioamide group 180° around the N^2–C^1 bond.

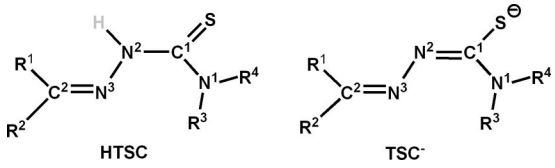

Scheme 1.

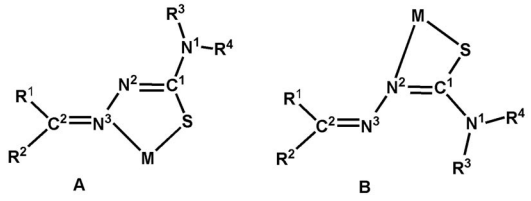

Scheme 2.

The isolation and structural identification of (*p*-anisaldehyde thiosemicarbazonato)dimethylthallium(III)[2]

[a] Departamento de Química Inorgánica, Facultade de Farmacia, Universidade de Santiago de Compostela, 15782 Santiago de Compostela, Galicia, Spain
Fax: +34-981-547102
E-mail: sergio.casas@usc.es
[b] Departamento de Química Física, Facultade de Química, Universidade de Santiago de Compostela, 15782 Santiago de Compostela, Galicia, Spain

Supporting information for this article is available on the WWW under http://dx.doi.org/10.1002/ejic.201000669.

showed that another coordination mode for the thiosemicarbazonate chain is possible, namely, N^2,*S*-chelation (**B**, Scheme 2). In this case, in which a less stable four-membered chelate ring is formed, large changes in the structure of the free ligand are not needed. Since this first example of N^2,*S*-chelation was described, more than forty complexes with coordination mode **B** have been identified by X-ray diffraction (CSD[3]) – although this number is still a very low percentage of all the thiosemicarbazonates studied to date.

There have been several attempts to rationalize the formation of a four-membered chelate ring instead of the more usual five-membered ring. For example, Bhattacharya et al.[4] suggested that the size of the C^2-substituent *trans* to N^2 (R^2, Scheme 1) determines the coordination mode, with the unusual N^2,*S*-coordination sterically favoured by the bulky R^2 groups. Subsequent contributions[5,6] support the idea that coordination may be determined by small differences in weak bonding interactions and/or by the steric requirements of the packing.

In the work described here, an analysis of the interaction between isatin-3-thiosemicarbazone (HL^1) and isatin-3-(N^1-methylthiosemicarbazone) (HL^2) with diphenyllead(IV) and lead(II) was carried out. The results shed new light on the coordination modes of the thiosemicarbazonate chain. Isatin-based thiosemicarbazones (Scheme 3) have very interesting chemotherapeutic properties[7] that, in some cases, are amplified by the presence of metal ions such as Cu^{II}.[8] Although the role of metal complexes in this amplification has been questioned,[9] it is somewhat surprising that very little attention has been payed to the coordination chemistry of isatin thiosemicarbazones in general and, in particular, to the structural characterization of their complexes. According to the limited information available, isatin-3-thiosemicarbazonates behave mainly as *O*,N^3,*S*-tridentate ligands,[10,11] although some N^3,*S*-chelates have also been identified.[12]

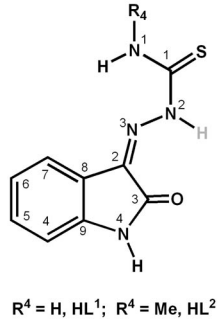

R^4 = H, HL^1; R^4 = Me, HL^2

Scheme 3.

The metal ions selected for this work ($PbPh_2^{2+}$ and Pb^{2+}) will result in HL^1 and HL^2 being confronted with two rather different coordination demands. Diorganolead(IV) cations are almost linear and bonding to the ligand is usually in the equatorial plane of a bipyramid; the R groups occupy the apical positions. The coordination of lead(II), however, clearly lacks the limitations associated with the presence of the R groups, but it is very often influenced by a stereochemically active lone electron pair that heavily restricts the spatial distribution of the Pb^{II}–ligand donor bonds.[13] In the present work it will therefore be possible to explore if the existence of significant differences in the steric demand of the metal centre can influence the *O*,N^2,*S*- or *O*,N^3,*S*-coordination mode adopted by the selected ligands (hereafter denoted N^2-L^x-coordination and N^3-L^x-coordination).

Results and Discussion

The complexes were obtained by adding a freshly prepared solution of $PbPh_2(OAc)_2$ or $Pb(OAc)_2{\cdot}3H_2O$ in methanol (see Exp. Section) to a solution of the corresponding thiosemicarbazone in ethanol or methanol. The [$PbPh_2$-(OAc)(L^x)] or [Pb(OAc)(L^x)] stoichiometry of the isolated complexes did not change when 1:1 and 2:1 ligand:metal molar ratios were used in the synthesis. No attempts were made to prepare the homoleptic [$PbPh_2(L^x)_2$] and [$Pb(L^x)_2$] complexes using molar ratios higher than 2:1.

The organolead(IV) derivatives were isolated as crystalline solids. In the case of [Pb(OAc)(L^1)], besides the previous formation of a microcrystalline orange precipitate with this composition, two types of single crystals were grown from the mother liquor: yellow-coloured prismatic crystals with the same stoichiometry as that of the former precipitate and octahedral-shaped orange crystals with the formula [Pb(OAc)(L^1)]·$3H_2O$.

Description of the Structures

$HL^2{\cdot}H_2O$

The structure and numbering scheme for this compound are shown in Figure 1 and the significant structural param-

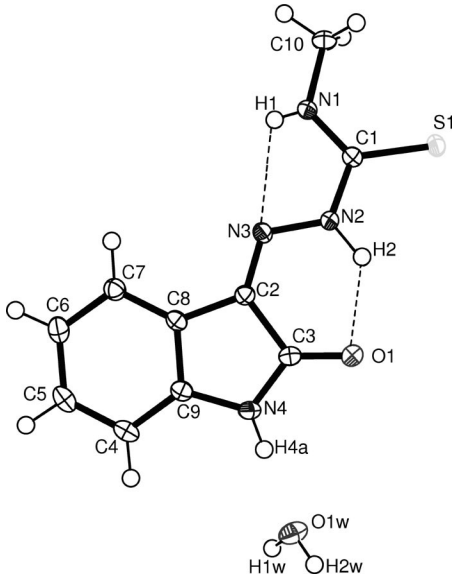

Figure 1. The crystal structure of $HL^2{\cdot}H_2O$ showing the intramolecular hydrogen bonds.

eters are listed in Table 1. The asymmetric unit consists of one molecule of thiosemicarbazone and one water molecule. The isatin moiety and the thiosemicarbazone backbone are both practically planar and form a dihedral angle of 9.73°. As in all examples of free isatin thiosemicarbazones studied to date by X-ray diffraction,[3] the configuration of HL^2 about the C(2)=N(3) bond is *Z*, probably because this arrangement permits the formation of the strong intramolecular hydrogen bond N(2)–H···O(1) (see Figure 1 and Table 2) and simultaneously avoids the steric hindrance between H(2) and H(7), which occurs in the *E* conformation (Scheme 4).[14] Furthermore, the sulfur atom is *trans* to N(3).

Table 1. Selected bond lengths [Å] and angles [°] in $HL^2 \cdot H_2O$.

S(1)–C(1)	1.6923(10)	C(2)–C(8)	1.4566(13)
O(1)–C(3)	1.2385(12)	C(2)–C(3)	1.5086(13)
N(1)–C(1)	1.3187(12)	C(4)–C(9)	1.3838(14)
N(1)–C(10)	1.4575(13)	C(4)–C(5)	1.3991(15)
N(2)–N(3)	1.3576(11)	C(5)–C(6)	1.3941(16)
N(2)–C(1)	1.3708(12)	C(6)–C(7)	1.3964(14)
N(3)–C(2)	1.2914(12)	C(7)–C(8)	1.3874(13)
N(4)–C(3)	1.3505(13)	C(8)–C(9)	1.4046(13)
N(4)–C(9)	1.4107(13)		
C(1)–N(1)–C(10)	122.96(9)	N(4)–C(3)–C(2)	106.64(8)
N(3)–N(2)–C(1)	119.98(8)	C(9)–C(4)–C(5)	117.05(9)
C(2)–N(3)–N(2)	116.29(8)	C(6)–C(5)–C(4)	121.57(10)
C(3)–N(4)–C(9)	110.92(8)	C(5)–C(6)–C(7)	120.83(10)
N(1)–C(1)–N(2)	117.03(9)	C(8)–C(7)–C(6)	118.03(9)
N(1)–C(1)–S(1)	125.25(8)	C(7)–C(8)–C(9)	120.59(9)
N(2)–C(1)–S(1)	117.72(7)	C(7)–C(8)–C(2)	133.02(9)
N(3)–C(2)–C(8)	126.21(9)	C(9)–C(8)–C(2)	106.31(8)
N(3)–C(2)–C(3)	127.41(9)	C(4)–C(9)–C(8)	121.92(9)
C(8)–C(2)–C(3)	106.22(8)	C(4)–C(9)–N(4)	128.19(9)
O(1)–C(3)–N(4)	127.19(9)	C(8)–C(9)–N(4)	109.88(8)
O(1)–C(3)–C(2)	126.16(9)		

Table 2. Hydrogen bonding parameters (Å, °) in $HL^2 \cdot H_2O$.

D–H···A[a]	*d*(D–H)	*d*(H···A)	*d*(D···A)	<(DHA)
N(1)–H(1)···N(3)	0.875(15)	2.251(14)	2.6489(12)	107.5(11)
N(1)–H(1)···S(1)^{i}	0.875(15)	2.620(15)	3.3999(9)	148.9(12)
O(1W)–H(1W)···S(1)^{ii}	0.839(19)	2.506(19)	3.3395(9)	172.6(16)
N(2)–H(2)···O(1)	0.838(15)	2.044(15)	2.7240(11)	137.9(14)
O(1W)–H(2W)···O(1)^{iii}	0.81(2)	1.99(2)	2.7987(11)	178.2(19)
N(4)–H(4A)···O(1W)	0.852(17)	1.933(17)	2.7764(12)	170.3(15)

[a] Symmetry operators, i: *x*, –*y* + 1/2, *z* – 1/2; ii: –*x* – 1, *y* + 1/2, –*z* + 3/2; iii: –*x* – 1, –*y* + 1, –*z* + 2.

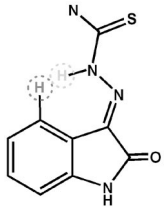

Scheme 4.

Although the C(1)–N(2) bond is formally a single bond, theoretical studies[15] indicate that there is a restricted rotation around it, so the observed mutual arrangement of S(1) and N(3) in $HL^2 \cdot H_2O$ can be labelled as the *E* configuration. The structure of this part of the thiosemicarbazone chain in free isatin thiosemicarbazones is not homogeneous in the solid state and both *Z* and *E* configurations have been identified.[3] Nevertheless, a close look at the available structures shows that the *Z* configuration occurs only when N(1) is fully substituted, probably because, if an N(1)–H group exists, the *E* configuration allows the formation of an additional intramolecular hydrogen bond [N(1)–H(1)··· N(3), see Figure 1 and Table 2]. This bond is not possible in the *Z* configuration.

There are several additional intermolecular hydrogen bonds in the compound (Table 2). One is formed between N(1)–H(1) and the S atom of another molecule [so H(1) is involved in a bifurcated hydrogen bond], which associates the molecules in chains along the *c* axis. Within the chain, the molecules are distributed into two planes that form a dihedral angle of ca. 118° (see Figure S1). The water molecule is involved in three hydrogen bonds (see Table 2), which connect the chains to give double layers in the *bc* plane stacked along the *a* axis (Figure 2).

$[PbPh_2(OAc)(N^2\text{-}L^1)]\cdot MeOH\cdot EtOH$ and $[PbPh_2(OAc)(N^3\text{-}L^2)]\cdot H_2O$

The molecular structure of the former complex is shown in Figure 3 and the most significant structural parameters are given in Table 3. The asymmetric unit consists of a mo-

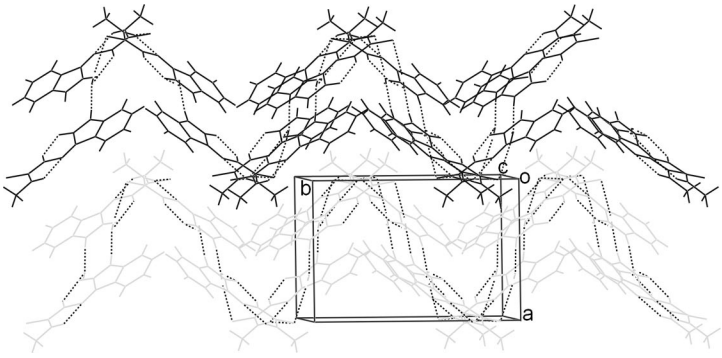

Figure 2. The double layers of $HL^2 \cdot H_2O$ stacked along the *a* axis.

lecule of the complex and one each of MeOH and EtOH. In $[PbPh_2(OAc)(N^2\text{-}L^1)]$, the $PbPh_2^{2+}$ moiety is bound to a monodeprotonated O,N^2,S-coordinated thiosemicarbazonate and to an anisobidentate acetate, both located on the equatorial plane of a distorted pentagonal bipyramidal coordination sphere in which the two phenyl groups are in apical positions. The main distortions affect the O(1)–Pb–O(3) and O(2)–Pb–O(3) angles – due to the small bite size of the ligands – and the C(20)–Pb–C(30) angle [156.58(16)°], which bends towards the equatorial position with less steric hindrance. As a result, this complex constitutes a new example of the rare N^2,S-coordination mode of the thiosemicarbazonate chain, and the isatin-3-thiosemicarbazonate forms with the metal atom a four- and a six-membered chelate ring.

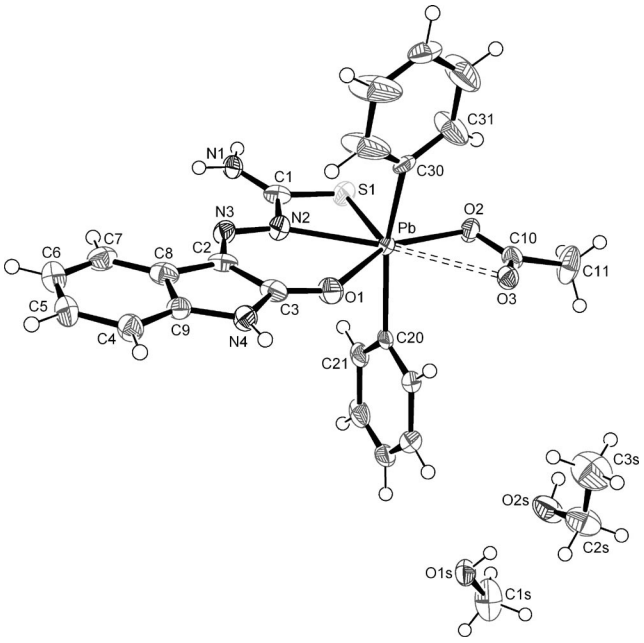

Figure 3. The molecular structure of $[PbPh_2(OAc)(N^2\text{-}L^1)]\cdot MeOH\cdot EtOH$.

Table 3. Selected bond lengths [Å] and angles [°] in $[PbPh_2(OAc)(N^2\text{-}L^1)]\cdot MeOH\cdot EtOH$.

Pb–C(20)	2.161(4)	N(4)–C(3)	1.361(5)
Pb–C(30)	2.172(4)	N(4)–C(9)	1.395(5)
Pb–O(2)	2.406(3)	C(2)–C(8)	1.456(6)
Pb–N(2)	2.433(4)	C(2)–C(3)	1.504(6)
Pb–O(1)	2.606(3)	C(4)–C(9)	1.381(6)
Pb–S(1)	2.6434(11)	C(4)–C(5)	1.386(6)
Pb···O(3)	2.803(3)	C(5)–C(6)	1.373(7)
S(1)–C(1)	1.724(5)	C(6)–C(7)	1.375(6)
O(1)–C(3)	1.229(5)	C(7)–C(8)	1.391(6)
O(2)–C(10)	1.282(5)	C(8)–C(9)	1.403(6)
O(3)–C(10)	1.247(5)	C(10)–C(11)	1.506(6)
N(1)–C(1)	1.317(6)	O(1S)–C(1S)	1.440(6)
N(2)–N(3)	1.339(5)	O(2S)–C(2S)	1.414(6)
N(2)–C(1)	1.363(5)	C(2S)–C(3S)	1.441(7)
N(3)–C(2)	1.330(5)		
C(20)–Pb–C(30)	156.58(16)	N(2)–Pb–O(1)	70.54(11)
O(2)–Pb–S(1)	75.70(7)	O(1)–Pb–O(3)	103.90(9)
N(2)–Pb–S(1)	60.24(9)	O(2)–Pb–O(3)	49.49(9)

When the structure of the isatin thiosemicarbazonate moiety in $[PbPh_2(OAc)(N^2\text{-}L^1)]$ is compared with that of HL^1,[12] it is evident that coordination did not induce significant changes in the configuration of the free ligand. There are some adjustments in bond lengths and angles [e.g., the length of C(1)–S(1) increases from 1.663(4) in free HL^1[12] to 1.724(5) Å in the complex, in accordance with the usual thione to thiol evolution in this type of complex] but the initial configuration of the thiosemicarbazone remains "frozen" during deprotonation, metallation and precipitation. This finding is quite consistent with the observed slow change in the configuration about the C(2)=N(3) bond when derivatives of HL^1 lose their proton in solution,[14] and also with the calculated partial double bond character of the N(2)–C(1) bond.[15] In the present case it appears that the N^2,S-coordination is the result of the slow conformational evolution of the ligand and of the sparing solubility of the N^2,S-bound complex, which precipitates before the donor atoms of the ligand can be rearranged appropriately to afford the N^3,S-coordination mode. Additionally, there are several weak bonding interactions in the lattice of the $[PbPh_2(OAc)(N^2\text{-}L^1)]\cdot MeOH\cdot EtOH$ compound (Table 4). A hydrogen bond [N(4)–H(4)···O(3)] links the molecules into dimers and these are connected in chains through the $N(1)H_2$ group and the oxygen atom of the methanol molecules (Figure S2). Finally, the chains are linked by the ethanol molecules and form stacked layers, as shown in Figure S3.

Table 4. Hydrogen bond parameters (Å, °) in $[PbPh_2(OAc)(N^2\text{-}L^1)]\cdot MeOH\cdot EtOH$.

D–H···A[a]	*d*(D–H)	*d*(H···A)	*d*(D···A)	<(DHA)
N(1)–H(1A)···O(1S)^{i}	0.86	2.31	2.944(5)	130.4
N(1)–H(1B)···O(1S)^{ii}	0.86	2.03	2.884(5)	173.5
O(1S)–H(1S)···O(2S)	0.82	1.85	2.674(5)	178.6
O(2S)–H(2S)···O(2)^{iii}	0.82	1.92	2.730(4)	169.7
N(4)–H(4)···O(3)^{iv}	0.86	1.95	2.789(5)	165.9
N(1)–H(1A)···N(3)	0.86	2.42	2.672(5)	97.7

[a] Symmetry operators, i: $-x + 2, -y + 1, -z + 1$; ii: $x, y, z + 1$; iii: $-x + 1, -y + 1, -z + 1$; iv: $-x + 1, -y + 2, -z + 1$.

The molecular structure of $[PbPh_2(OAc)(N^3\text{-}L^2)]\cdot H_2O$ and the numbering scheme used are shown in Figure 4; the most relevant bond lengths and angles are given in Table 5. As in the $(L^1)^-$ complex, the $PbPh_2^{2+}$ unit is bound to an anisobidentate acetate and a tridentate thiosemicarbazonate, both located on the equatorial plane of a distorted pentagonal bipyramid in which the Ph groups are the apices. Unlike the coordination mode exhibited by $(L^1)^-$ in $[PbPh_2(OAc)(N^2\text{-}L^1)]\cdot MeOH\cdot EtOH$, $(L^2)^-$ is O,N^3,S-coordinated and forms two five-membered chelate rings with the metal. To achieve this, the configuration of HL^2 must be strongly modified after deprotonation (see Figures 1 and 4). Specifically, the configuration around the C(1)–N(2) bond must change from *E* to *Z* and that around C(2)=N(3) from *Z* to *E*, both by rotating 180° about the respective bonds. The former change implies, in addition to overcoming the rotational barrier due to the partial multiplicity of the bond, the breaking of the N(1)–H···N(3) intramolecular

hydrogen bond. The change around the C(2)=N(3) bond is not affected by the other intramolecular hydrogen bond [N(2)–H···O(1)] because it disappears when HL^2 is deprotonated. The molecules of the complex and those of the water interact in the lattice through hydrogen bonds that involve the oxygen atoms of the acetate and the water molecule and the N(1)–H, N(4)–H and O(1 W)–H groups (see Table 6). The N(4)–H(4)···O(3)^{ii} bond links the [$PbPh_2(OAc)(N^3$-$L^2)$] molecules to give dimers that, in turn, interact through the water molecules to form chains packed as shown in Figure 5. The π-π stacking interactions between the phenyl groups of the organometal moiety (distance between centroids ($C_{30–35}$) is 3.875 Å) assemble these chains into a 2D-network (Figure 5).

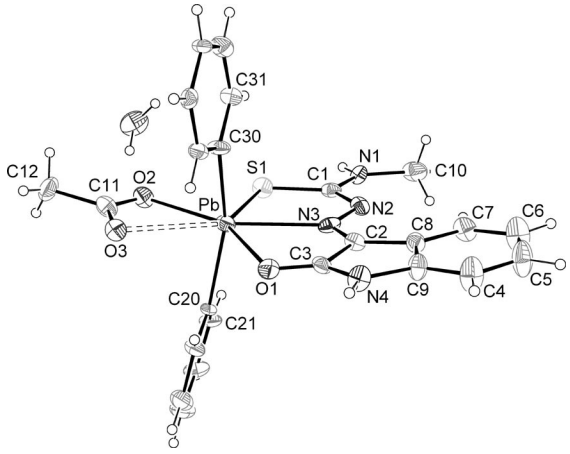

Figure 4. The molecular structure of [$PbPh_2(OAc)(N^3$-$L^2)$]·H_2O.

Table 5. Selected bond lengths [Å] and angles [°] in [$PbPh_2(OAc)(N^3$-$L^2)$]·H_2O.

Pb–C(20)	2.212(15)	N(2)–N(3)	1.35(2)
Pb–C(30)	2.205(16)	N(3)–C(2)	1.29(2)
Pb–O(2)	2.431(12)	N(4)–C(3)	1.33(2)
Pb–N(3)	2.523(15)	N(4)–C(9)	1.41(2)
Pb–S(1)	2.596(4)	C(3)–C(2)	1.47(2)
Pb–O(1)	2.686(12)	C(2)–C(8)	1.47(2)
Pb–O(3)	2.743(12)	C(4)–C(9)	1.37(3)
S(1)–C(1)	1.757(18)	C(4)–C(5)	1.38(3)
O(1)–C(3)	1.232(19)	C(5)–C(6)	1.42(3)
O(2)–C(11)	1.26(2)	C(6)–C(7)	1.39(3)
O(3)–C(11)	1.24(2)	C(7)–C(8)	1.39(2)
N(1)–C(1)	1.33(2)	C(8)–C(9)	1.43(2)
N(1)–C(10)	1.45(2)	C(11)–C(12)	1.54(3)
N(2)–C(1)	1.36(2)		
C(20)–Pb–C(30)	154.1(7)	N(3)–Pb–O(1)	65.2(4)
O(2)–Pb–S(1)	78.9(3)	O(1)–Pb–O(3)	94.6(4)
N(3)–Pb–S(1)	71.7(4)	O(2)–Pb–O(3)	49.8(4)

Table 6. Hydrogen bonding parameters (Å, °) in [$PbPh_2(OAc)(N^3$-$L^2)$]·H_2O.

D–H···A[a]	*d*(D–H)	*d*(H···A)	*d*(D···A)	<(DHA)
N(1)–H(1)···O(1W)^{i}	0.86	1.96	2.81(2)	174.4
O(1W)–H(1W)···O(2)	0.858(15)	1.952(12)	2.750(19)	154.2(12)
N(4)–H(4)···O(3)^{ii}	0.86	1.88	2.741(18)	176.6

[a] Symmetry operators, i: –*x*, –*y* + 1, –*z* + 1; ii: –*x*, –*y*, –*z*.

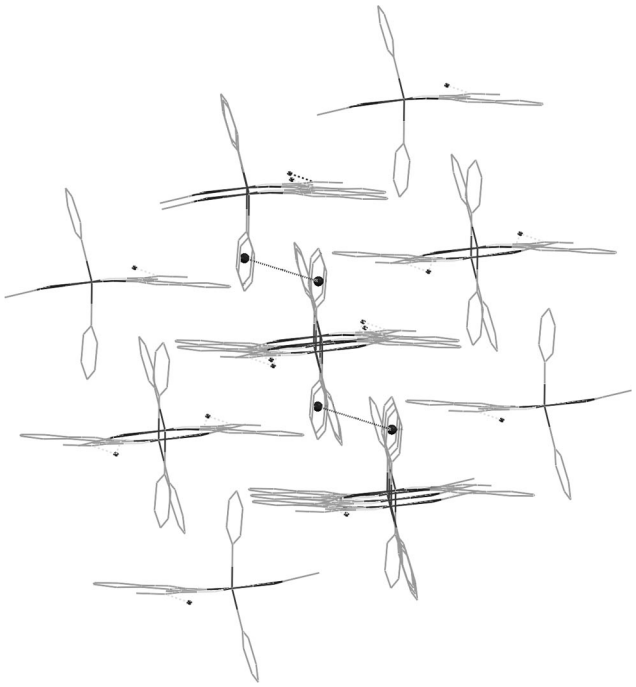

Figure 5. The distribution of the chains formed by hydrogen bonding interactions in the lattice of [$PbPh_2(OAc)(N^3$-$L^2)$]·H_2O, and the π-π stacking interactions.

[Pb(OAc)(N^2-L^1)] and [Pb(OAc)(N^3-L^1)]·3H_2O

The structures of these complexes are presented in Figure 6 and the relevant bond lengths and angles are listed in Table 7. Both derivatives were obtained from the mother liquor of the same reaction after slow evaporation of the solvent at room temperature. The complex [Pb(OAc)(N^2-L^1)] evolved as abundant but very small prismatic yellow crystals, whereas [Pb(OAc)(N^3-L^1)]·3H_2O crystallized as a small number of octahedral bright-orange crystals.

As shown in Figure 7, [Pb(OAc)(N^2-L^1)] and [Pb(OAc)-(N^3-L^1)] are linkage isomers with the thiosemicarbazonate ligand *O*,N^2,*S*-coordinated in the former and *O*,N^3,*S*-coordinated in the latter. The coordination sphere of lead(II) in both complexes is rather irregular. The void in the distribution of the bonds around the metal suggests the presence of a stereochemically active lone electron pair (hemidirected coordination[16]). In [Pb(OAc)(N^2-L^1)], if the very weak bonding interactions are ignored, the coordination sphere can be roughly described as a square pyramid with a vacant basal position and the two O atoms of the acetate sharing the apical position due to the narrow bite of this ligand (Figure 7, a). In [Pb(OAc)(N^3-L^1)]·3H_2O, again only taking into account the most significant bonds, the stereochemical arrangement around the metal (Figure 7, b) is also a square pyramid with a vacant basal position but, in this case, only one O atom occupies the apex because the acetate is practically monodentate. As with the diphenyllead(IV) derivatives (see Tables 3 and 5), there are clear differences between the Pb–N bond lengths of the two isomers, this distance being shorter in the N^2-bound than in the N^3-bound complex. In the latter case, the relaxation of this bond is accompanied

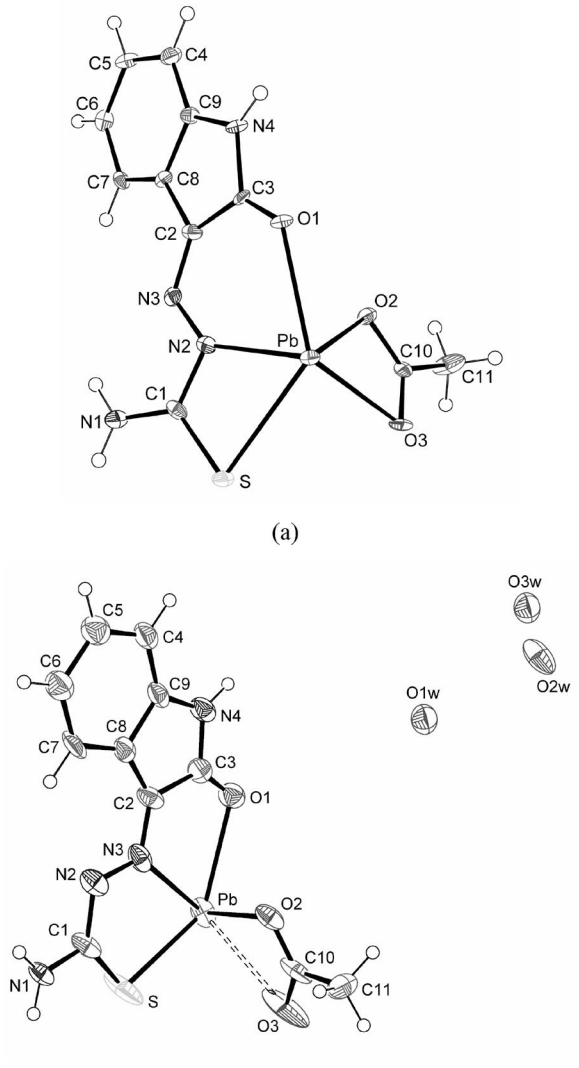

Figure 6. The molecular structures of (a) [Pb(OAc)(N^2-L^1)] and (b) [Pb(OAc)(N^3-L^1)]·3H_2O.

by a reinforcement of the Pb–S bond and, as the sulfur displaces toward the Pb^{II} atom, the isatin oxygen atom moves away from the metal, thus increasing the Pb···O(1) distance. Therefore, the bonding system in [Pb(OAc)(N^3-L^1)]·3H_2O is quite similar to that in the homoleptic complex [Pb(Ishewim)$_2$] [HIshewim = isatin-3-(hexamethyleneiminyl-thiosemicarbazone)],[11] although the bond lengths are slightly shorter.

In [Pb(OAc)(N^2-L^1)], each molecule forms two weak Pb···O interactions with neighbouring molecules to form chains along the *a* axis. These chains are associated into a 3D-lattice through intermolecular N(1)–H(1B)···O(2)^{i} and N(4)–H(4)···O(3)^{ii} hydrogen bonds (see Table 8 and Figure S4).

The lattice of [Pb(OAc)(N^3-L^1)]·3H_2O is more complex. The weak intermolecular Pb···S bond (see Figure 7, b) and the N(1)–H(1B)···O(3)^{ii} hydrogen bond (Table 8) assemble the molecules into tetramers (Figure S5). These tetramers

Table 7. Selected bond lengths [Å] and angles [°] in [Pb(OAc)(N^2-L^1)] and [Pb(OAc)(N^3-L^1)]·3H_2O.

	[Pb(OAc)(N^2-L^1)][a]	[Pb(OAc)(N^3-L^1)]·3H_2O[a]
Pb–O(1)	2.560(5)	2.700(6)
Pb–O(2)	2.444(5)	2.382(5)
Pb–O(3)	2.697(5)	2.946(11)
Pb–N(2)	2.385(6)	
Pb–N(3)		2.535(7)
Pb–S	2.860(2)	2.665(3)
Pb···S^{i}		3.343(2)
Pb···O3^{ii}	3.038(5)	
Pb···O1^{iii}	3.196(4)	
S–C(1)	1.701(8)	1.691(9)
O(1)–C(3)	1.245(8)	1.241(10)
O(2)–C(10)	1.270(8)	1.282(11)
O(3)–C(10)	1.241(9)	1.229(10)
N(1)–C(1)	1.330(9)	1.325(10)
N(2)–N(3)	1.344(8)	1.344(9)
N(2)–C(1)	1.365(9)	1.364(10)
N(3)–C(2)	1.310(9)	1.340(10)
N(4)–C(3)	1.378(9)	1.367(11)
N(4)–C(9)	1.395(8)	1.398(11)
N(2)–Pb–O(1)	72.97(16)	
N(2)–Pb–S	58.60(14)	
N(3)–Pb–S		68.27(16)
O(2)–Pb–O(1)		78.31(18)
N(3)–Pb–O(1)		66.0(2)
O(2)–Pb–O(3)	50.39(15)	47.66(19)
O(3)–C(10)–O(2)	122.5(7)	123.6(11)

[a] Symmetry operators, i: 0.25 + *y*, 0.75 – *x*, 0.75 – *z*; ii: –*x* + 2, –*y*, –*z*; iii: –*x* + 1, –*y*, –*z*.

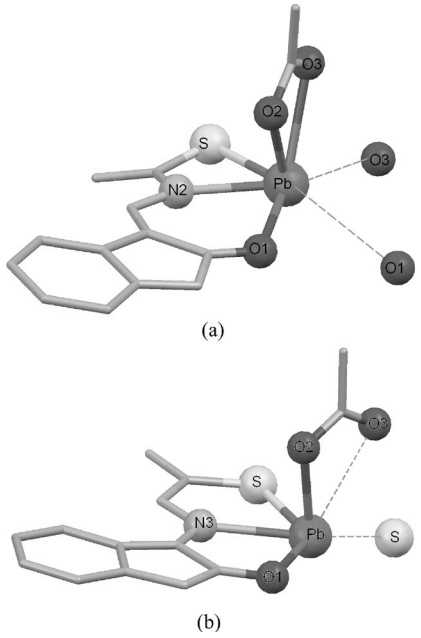

Figure 7. The coordination spheres of lead(II) in (a) [Pb(OAc)(N^2-L^1)] and (b) [Pb(OAc)(N^3-L^1)]·3H_2O.

interact through the N(1)–H(1A)··O(2)^{i} hydrogen bond to form the 3D arrangement shown in Figure S6. The water molecules are placed in the void spaces of this arrangement and, as it was not possible to locate their hydrogen atoms, the association of these molecules must be described on the

Table 8. Hydrogen bonding parameters (Å, °) in [Pb(OAc)(N^2-L^1)] and [Pb(OAc)(N^3-L^1)]·3H_2O.

D–H···A	*d*(D–H)	*d*(H···A)	*d*(D···A)	<(DHA)
[Pb(OAc)(N^2-L^1)][a]				
N(1)–H(1A)···N(3)	0.86	2.30	2.610(9)	101.4
N(1)–H(1B)···O(2)^{i}	0.86	2.02	2.858(8)	163.7
N(4)–H(4)···O(3)^{ii}	0.86	2.00	2.845(7)	167.3
[Pb(OAc)(N^3-L^1)]·3H_2O[b]				
N(1)–H(1A)···O(2)^{i}	0.86	2.15	2.941(9)	153.5
N(1)–H(1B)···O(3)^{ii}	0.86	1.97	2.823(9)	173.3
O(1 W)···O(1 W)^{iii}			2.778(9)	
O(2 W)···O(1 W)			2.853(9)	
O(2 W)···O(2)^{iii}			2.797(8)	
O(3 W)···O(2 W)			2.739(9)	
N(4)–H(4)···O(3 W)^{iv}	0.86	2.01	2.865(9)	172.9
O(3 W)···O(1 W)^{iii}			2.792(8)	
O(3 W)···O(3 W)^{v}			2.788(12)	

[a] i: *x*, –*y* + 1/2, z – 1/2, ii: *x* – 1, *y*, *z*. [b] i: –*x* + 1/2, –*y* + 1/2, –*z* + 1/2; ii: –*y* + 3/4, *x* – 1/4, –*z* + 3/4; iii: *y* – 1/4, –*x* + 5/4, –*z* + 1/4; iv = –*x* + 1, –*y* + 3/2, *z* + 0, v = –*x* + 1, –*y* + 2, –*z*.

basis of the O···O distances (see Table 8). The water molecules arrange to form a dodecameric $(H_2O)_{12}$ cluster; this type of cluster has previously been observed[17] but, as far as we know, the saddle-shaped form detected in the present case (Figure 8, a) is new. The distances between the oxygen atoms range from 2.739 to 2.853 Å, with the shorter distances associated with the four O(2 W)···O(3 W) bonds of the saddle. The lower limit of the range is close to that of hexagonal ice (2.75 Å[18]) and, in general, these O···O distances are a little shorter than in other dodecameric clusters.[17] This structure can be considered to be a modification of the fused-cube structure[19] in which the faces of the two cubes opposite to those fused are partially opened, possibly to allow additional interactions of the cluster with the molecules of the complex and with the neighbouring clusters. The first interactions (Table 8 and Figure 8, b) connect O(3 W) with the N(4)–H(4) group from the isatin pentagonal ring and O(2 W) with the oxygen from the acetate [O(2)] bound to the metal in the complex. Additionally, the interaction of the cluster with neighbouring $(H_2O)_{12}$ entities through O(3 W)···O(3 W)^{v} interactions (2.788 Å) links the water molecules in a 3D sub-lattice (Figure 8, c).

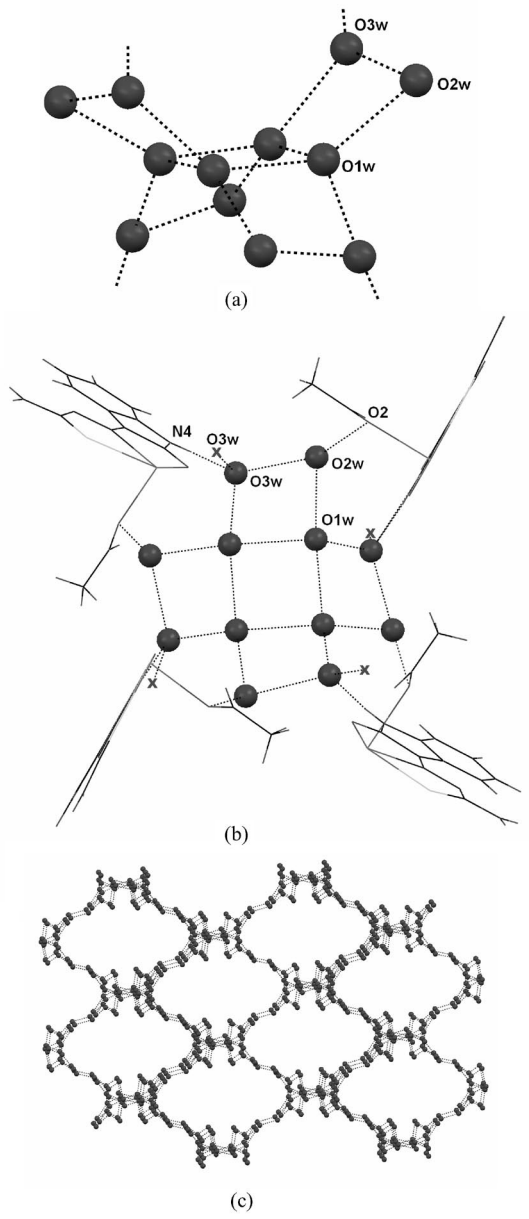

Figure 8. The $(H_2O)_{12}$ cluster in the crystal of [Pb(OAc)(N^3-L^1)]·3H_2O showing: (a) the saddle-shaped form; (b) the hydrogen bonds with the molecules of complex and the connections with neighbouring clusters through O(3 W)···O(3 W) interactions (x); and (c) the final 3D-arrangement of the water molecules.

NMR Spectroscopy

The results discussed above do not shed much light on the factors that determine the N^2- and N^3-coordination modes. In fact, the study of the diphenyllead(IV) complexes seems to suggest that small modifications in the N(1) substituents in the thiosemicarbazonate ligand could determine the adopted mode, whereas the behaviour of the Pb^{II}/HL^1 system indicates that both coordination modes coexist in the synthetic reaction. Therefore, to further clarify this matter, we decided to perform ^{1}H and ^{13}C NMR spectroscopic solution studies. For solubility reasons, the spectra were measured in [D_6]DMSO instead of methanol, the solvent that we used to prepare the complexes in the solid state. The appropriateness of this approach is supported by the fact that both solvents afford similar ^{1}H NMR spectra for selected samples. The NMR spectroscopic data are given in the Experimental Section.

In the ^{1}H NMR spectra of HL^1 and HL^2, the most relevant signals from the coordination point of view are that of N(2)–H ($\delta \approx 12.5$ ppm) and C(7)–H ($\delta \approx 7.6$ ppm) (see the numbering scheme in Figure 1). The former signal disappeared on formation of the complexes in accordance with deprotonation of the ligand, and the second signal was very sensitive to the coordination mode of the ligands (see be-

low). Deprotonation and metallation also affect the resonances of C(1), C(2), C(3) and C(7), which occur at $\delta \approx 178$, 132, 163 and 121 ppm, respectively, in the ^{13}C NMR spectra of the free ligands.

The spectra of the complexes usually contain a higher number of signals than expected, suggesting the presence of more than one species in solution – presumably isomeric derivatives. Thus, in the ^{1}H and ^{13}C NMR spectra of [Pb(OAc)(L^1)], two doublets associated with the C(7)–H proton and two signals for some of the carbons from the ligand, including the C(7) carbon were observed. The isolation and full characterization in solid state of the two isomers in the case of complex [Pb(OAc)(L^1)] allowed, using freshly prepared solutions, the identification of the signals of both isomers and the subsequent analysis of the influence of the two coordination modes on the ligand spectra.

The best "fingerprint" in the ^{1}H NMR spectrum to identify the N^2 and the N^3 isomer is the doublet associated with the proton bound to C(7). This signal appears at δ = 7.65 ppm in HL^1 but is displaced to δ = 7.72 ppm in the N^2-bound isomer and to δ = 8.27 ppm in the N^3-coordinated complex. The different deshielding of C(7)–H in the two isomers is probably due to a nonequivalent influence of the magnetic anisotropy associated with the π-charge of the hydrazinic bond. Although this bond is formally represented as a single bond (Schemes 1 and 2), thiosemicarbazones have an extensively delocalized system[20] so the N(2)–N(3) bond possesses a partial double bond character, as confirmed by our DFT study (see below). Unlike the N^2 isomer, in the N^3 isomer this bond is situated close to C(7)–H and therefore causes deshielding of this proton.

In the ^{13}C NMR spectra, besides the differences in the position of the C(7) signal, some other carbon signals are also modified on changing the coordination mode of the ligand. For example C(1), which is always deshielded with respect to the corresponding carbon in the free ligand ($\delta \approx$ 178 ppm), is at lower field in the N^3 isomer than in the N^2 isomer {δ = 183.0 ppm in [Pb(OAc)(N^2-L^1)] and δ = 187.0 ppm in [Pb(OAc)(N^3-L^1)]}. In addition, the C(3) nucleus, the signal of which is at $\delta \approx$163 ppm in the free ligand, is shielded in the N^2,S isomer {δ = 158.6 ppm in [Pb(OAc)(N^2-L^1)]} and deshielded in the N^3,S isomer {δ = 168.1 ppm in [Pb(OAc)(N^3-L^1)]}. The behaviour of the C(1) resonance can be rationalized by considering that the inductive influence of the metal should be more important in the N^3 isomer, because the shorter S–metal bond distance in this isomer suggests a stronger interaction. The more complex behaviour of C(3) may be due to the confluence of the induction provoked by the O(3)-metal interaction and the loss of the strong intramolecular N(2)–H···O(3) hydrogen bond.

Taking into account the behaviour of the C(7)–H signal in the ^{1}H NMR spectrum of a freshly prepared solution of [Pb(OAc)(L^2)], this complex, which was not studied by X-ray diffraction, is isolated as the [Pb(OAc)(N^2-L^2)] isomer.

Once the N^2- and N^3 isomers were identified from the NMR spectra, it was possible to analyze the evolution of these systems with time. This type of analysis helped to further clarify the findings in the solid state. The evolution of the spectrum of [Pb(OAc)(N^2-L^1)] with time is shown in Figure 9 and is particularly illustrative of the point outlined above. The first plot (t = 0) is of the solid isolated by concentrating the reaction solution after only 3 h under reflux. Although the presence of a small quantity of the N^3,*S* isomer cannot be ruled out because its signal may be masked by the strong broad signal associated with the $N(1)H_2$ group, it is evident that the N^2 isomer predominates in this first solution. This situation is reasonable considering the short reaction time and the slow structural evolution of this type of ligand on deprotonation.[14] When the spectrum of the same solution was recorded after two days, the signals of both isomers were observed with the predominance of the N^3-coordinated complex. It is worth noting that after one week some N^2 isomer still remains, but most of the complex is the N^3 isomer. After one week, no further significant evolution occurs (Figure 9).

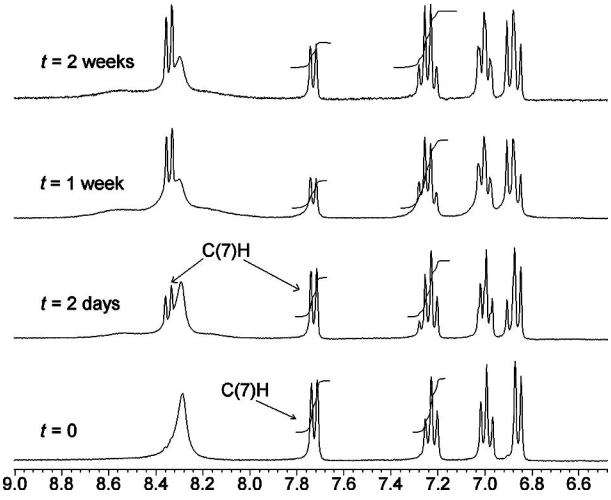

Figure 9. The evolution of the ^{1}H NMR spectrum of the [Pb(OAc)(L^1)] complex with time (see text for details).

Therefore, as the solid state study also suggested, the evolution of these complexes in solution is as follows: i) if the reaction time is short or the initially formed complex is insoluble, the N^2 *isomer* is isolated; and ii) when the reaction time increases or the complex is kept in solution for a long period, the solid formed is mostly the N^3 derivative, which is probably the thermodynamically controlled product.

This conclusion is also supported by the behaviour of [$PbPh_2$(OAc)(L^1)]. When the solution obtained in the synthesis of this complex was immediately concentrated, the isolated solid mainly corresponded to the N^2 *isomer* (see the ^{1}H NMR spectroscopic data, Experimental Section). When the solution was concentrated one week after the synthetic reaction, the spectral fingerprints of the product, however, mainly corresponded to the N^3 derivative.

The spectra of the $(L^2)^-$ compounds are more complex than those of $(L^1)^-$, suggesting the presence of more than two non-equivalent species from the spectroscopic viewpoint. In an effort to explain this finding, one can speculate

that the changes in the configuration of the ligand may not be simultaneous in the $(L^2)^-$ complexes when it evolves from the N^2 *isomer* to the N^3 isomer [rotation about the C(1)–N(1) and C(2)–N(3) bonds], thus leading to intermediate stages (such as that shown in Scheme 5) that are stable enough to be detected. This proposal is plausible because the methyl group on N(1) probably influences the strength of the N(1)–H···N(3) hydrogen bond, which must be broken to allow rotation around C(1)–N(2), however, the idea was not explored further.

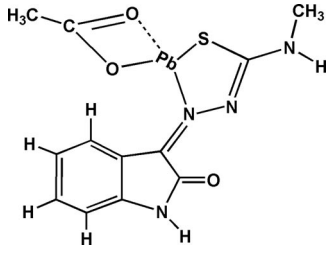

Scheme 5.

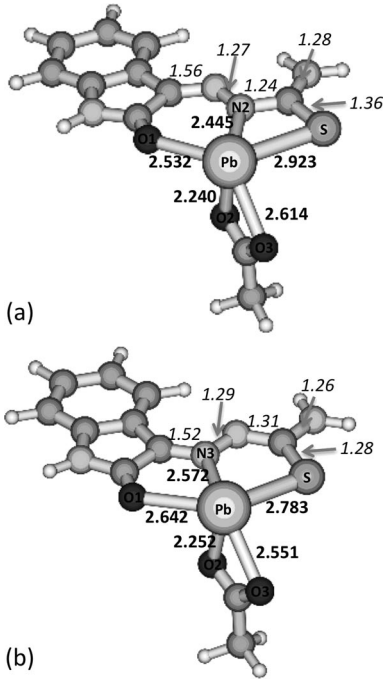

Figure 10. The gas-phase optimized conformations for (a) [Pb(OAc)(N^2-L^1)] and (b) [Pb(OAc)(N^3-L^1)]. Bond lengths involving the Pb atom are given in Å (numbers in bold). Bond orders for the bonds of the thiosemicarbazone chain are in italic.

DFT Calculations

The gas-phase structures of [Pb(OAc)(N^2-L^1)] and [Pb(OAc)(N^3-L^1)] optimized in this study by DFT calculations are depicted in Figure 10. The Figure shows the interatomic distances between the Pb ion and the ligand atoms, as well as the bond orders of the bonds associated with the thiosemicarbazone chain. As can be seen, the gas-phase conformations retain the most relevant geometrical features observed in the X-ray structures (see below). Thus, the Pb–S distance in [Pb(OAc)(N^2-L^1)] (2.923 Å) is substantially longer than that calculated for [Pb(OAc)(N^3-L^1)] (2.783 Å), as also observed in the solid state. In addition, the Pb–O(1) and Pb–N [N(2) or N(3)] distances in [Pb(OAc)(N^2-L^1)] (2.532 Å and 2.445 Å, respectively) are significantly shorter than those in [Pb(OAc)(N^3-L^1)] (2.642 Å and 2.572 Å, respectively). In both complexes, the calculated Pb–O(2) lengths are markedly shorter that the Pb–O(3) ones, showing a more pronounced anisobidentate character of the acetate ligand than that found in the solid state. Note that, despite all these differences, the agreement between experimental and theoretical studies are rather good considering that the latter do not take into account the presence of the intermolecular hydrogen bonds and packing forces in the crystal structures.

The calculations show that electron delocalization along the thiosemicarbazone chain is substantial (see bond orders in Figure 10). It is also noteworthy that the bond order predicted for the C–S bond in [Pb(OAc)(N^2-L^1)] (1.36) is higher than that in [Pb(OAc)(N^3-L^1)] (1.28). This suggests that the sulfur atom in the latter structure has more thiol character, which correlates with a stronger interaction with the Pb metal (i.e., shorter S–Pb bond length). Also of interest is the fact that the N(2)–C(1) bond order in the [Pb(OAc)(N^2-L^1)] complex (1.24) is lower than the corresponding bond order in [Pb(OAc)(N^3-L^1)] (1.31).

The DFT calculations predict that, in the gas phase, the energies of the two complexes are very similar to each other, although [Pb(OAc)(N^3-L^1)] is more stable than [Pb(OAc)(N^2-L^1)] by 0.6 kcal/mol. This is a rather small difference when compared with the results of similar DFT calculations on some benzaldehyde thiosemicarbazone complexes of ruthenium(II)[6] and explains the simultaneous isolation of both isomers in the present study.

The free energies of the two complexes in the gas phase at 298.15 K were also evaluated. The difference between ΔG values of [Pb(OAc)(N^3-L^1)] and [Pb(OAc)(N^2-L^1)] is calculated to be 0.8 kcal/mol, which gives an isomeric equilibrium constant of 3.79, favouring the formation of [Pb(OAc)(N^3-L^1)]. In dimethylsulfoxide, the DFT calculations with the PCM model predict that the difference between the ΔG values is 2.0 kcal/mol, suggesting that the formation of [Pb(OAc)(N^3-L^1)] is also favoured in this solvent.

Conclusion

In summary, in the complexes of isatin-3-thiosemicarbazones with $PbPh_2^{2+}$ and Pb^{2+} metal cations, although the N^3-chelated complex is thermodynamically more stable, the difference in stability with the N^2-chelated isomer is probably small. Additionally, the initial configuration of the isatin 3-thiosemicarbazone ligand, and its slow evolution from the *E*,*Z* to *Z*,*E* configuration with respect to the C(1)–N(2) and C(2)=N(3) bonds in solution, favoured the initial formation of the N^2 isomer as the kinetically controlled product. In accordance with this type of control, if the N^2 isomer does

not precipitate and remains in solution, it evolves with time – albeit not completely – to the more stable N^3 isomer (the thermodynamically controlled product). This incomplete transformation of the initial product and the slow isomeric transition allow the presence of both complexes in solution. This situation also permits the isolation of pure or mixed solids depending on the reaction time and the solubility of the complexes.

It seems plausible that all *N*,*S*-bonded thiosemicarbazones react with the metal ions as the isatin-3-thiosemicarbazone does. In most cases, however, the kinetically controlled N^2 isomer probably evolves to form the N^3 isomer so quickly that only the second is detected. The N^2 isomer is identified only when the electronic and steric influences of the R^1–R^4 substituents (see Scheme 1) slow down the conformational changes in the thiosemicarbazone chain.

Experimental Section

General: Thiosemicarbazide (Merck), 4-methyl-3-thiosemicarbazide (Aldrich), 2,3-indolinedione (isatin; Aldrich), silver acetate (Fluka), lead(II) acetate trihydrate (Probus), diphenyllead(IV) dichloride (ABCR), all of reagent grade, were used without further purification. Diphenyllead(IV) diacetate was prepared by reacting diphenyllead(IV) dichloride and silver acetate in methanol. The AgCl was removed by filtration and the solution containing organolead(IV) acetate was used immediately in the preparation of the complexes.

Elemental analyses for C,H,N and S were performed with a Fisons 1108 microanalyser. Melting points were determined with a Büchi melting point apparatus. NMR spectra were recorded in [D_6]-DMSO using Varian Mercury 300 and Varian Inova 500 spectrometers. The ^{1}H NMR spectra (at 300.14 or 500.14 MHz) and ^{13}C NMR spectra (75.4 or 125.76 MHz) are referenced to TMS by using the solvent signals: ^{1}H, 2.50 ppm; ^{13}C, 39.50 ppm. HMQC and HMBC experiments were also carried to confirm the assignments. Elemental analyses, spectroscopic measurements and X-ray data collection were carried out in the RIAIDT services of the University of Santiago de Compostela.

Ligands: The isatin 3-thiosemicarbazones HL^1 and HL^2 were prepared according to the previously described method for HL^1 [12] by reacting isatin and the corresponding thiosemicarbazide, in a 1:1 molar ratio, in an ethanol/water solvent mixture.

HL^1: Yellow solid; yield 55%. $C_9H_8N_4OS$ (220.25): calcd. C 49.08, H 3.66, N 25.44, S 14.56; found C 49.64, H 3.89, N 25.92, S 15.19. ^{1}H NMR ([D_6]DMSO): δ = 12.47 [s, 1 H, N(2)H], 11.19 [s, 1 H, N(4)H], 9.04, 8.67 [s, 2 H, N(1)H_2], 7.65 [d, 1 H, C(7)H], 7.35 [t, 1 H, C(5)H], 7.08 [t, 1 H, C(6)H], 6.92 [d, 1 H, C(4)H] ppm. ^{13}C NMR ([D_6]DMSO): δ = 178.6 (C1), 162.6 (C3), 143.3 (C9), 132.0 (C2), 131.2 (C5), 122.3 (C6), 120.9 (C7), 119.9 (C8), 111.0 (C4) ppm.

HL^2: Yellow solid; yield 60%. $C_{10}H_{10}N_4OS$ (234.28): calcd. C 51.27, H 4.30, N 23.91, S 13.68; found C 51.04, H 4.31, N 23.70, S 13.40. ^{1}H NMR ([D_6]DMSO): δ = 12.59 [s, 1 H, N(2)H], 11.20 [s, 1 H, N(4)H], 9.24 [q, 1 H, N(1)H], 7.63 [d, 1 H, C(7)H], 7.35 [t, 1 H, C(5)H], 7.08 [t, 1 H, C(6)H], 6.93 [d, 1 H, C(4)H], 3.08 [d, 3 H, C(10)H_3] ppm. ^{13}C NMR ([D_6]DMSO): δ = 177.5 (C1), 162.5 (C3), 142.1 (C9), 131.5 (C2), 131.0 (C5), 122.2 (C6), 120.5 (C7), 119.9 (C8), 111.0 (C4), 31.2 (C10) ppm. Monocrystals of $HL^2{\cdot}H_2O$ suitable for X-ray diffraction were isolated from the mother liquor.

Complexes: The complexes were prepared by reacting the thiosemicarbazone with diphenyllead(IV) acetate or lead(II) acetate trihydrate in 1:1 and 1:2 molar ratios. The results were similar in both cases so only the 1:1 reactions are described.

[$PbPh_2(OAc)(L^1)$]: A solution of diphenyllead(IV) acetate (0.435 g, 0.90 mmol) in methanol (50 mL) was slowly added to a solution of HL^1 (0.200 g, 0.90 mmol) in ethanol (20 mL). The yellow solution was stirred and heated under reflux for 3 h. The mixture was cooled to r.t. and the volume of the solution was partially reduced until an orange crystalline solid appeared. The solid was removed by filtration; yield 31%, m.p. 203 °C (dec.). $C_{25}H_{26}N_4O_4PbS$ {[$PbPh_2(OAc)(L^1)$]·EtOH} (685.77): calcd. C 43.79, H 3.82, N 8.17, S 4.68; found C 42.30, H 3.56, N 8.15, S 4.69. ^{1}H NMR ([D_6]-DMSO): δ = 11.06 [br. s, 1 H, N(4)H], 9.00, 8.90, 8.60 [br. s, 2 H, N(1)H_2], *8.30*, 7.71 [d, 1 H, C(7)H], 7.85 [d, ^3J(^{1}H-^{207}Pb) = 194 Hz, 4 H, $H_{o\text{-}Ph}$)], 7.52, *7.48* (t, 4 H, $H_{m\text{-}Ph}$), 7.35, *7.34* (t, 2 H, $H_{p\text{-}Ph}$), *7.26*, 7.24 [t, 1 H, C(5)H], *7.02*, 7.01 [t, 1 H, C(6)H], *6.85*, 6.81 [d, 1 H, C(4)H], 4.34 (s, 1 H, OH_{EtOH}), 3.22 (q, 2 H, CH_2, EtOH), 1.78 (s, 3 H,CH_3, OAc), 1.06 (t, 3 H, CH_3, EtOH) ppm. ^{13}C NMR ([D_6]DMSO): δ = *182.5*, 178.8 (C1), 179.5 (COO), 166.8 ($C_{i\text{-}Ph}$), *166.4*, 159.6 (C3), *141.0*, 140.5 (C9), *136.6*, 136.2 (C2), 132.6 [^2J(^{13}C-^{207}Pb) = 119 Hz, $C_{o\text{-}Ph}$], 130.9, 128.9 (C5), 130.1, *130.0* [^3J(^{13}C-^{207}Pb) = 193 Hz, $C_{m\text{-}Ph}$], 129.4 ($C_{p\text{-}Ph}$), *126.2*, 120.3 (C7), 122.2 (C6), 121.9, *117.1* (C8), *110.8*, 110.5 (C4), 56.1 (CH_2, EtOH), 23.5 (CH_3, OAc), 18.6 (CH_3, EtOH) ppm. Here and hereafter the italicized signals correspond to a minor product. A monocrystal composed of **[$PbPh_2(OAc)(N^2$-$L^1)$]·MeOH·EtOH** suitable for an X-ray diffraction study was selected from the isolated crystalline solid. This solid easily lost the alcohol molecules justifying the slightly low value for the experimental C percentage.

A second reaction was carried out under similar conditions and the resulting solution was not concentrated immediately but one week later. An orange solid formed and was removed by filtration, vacuum dried and subjected to elemental analysis and ^{1}H NMR spectroscopy. $C_{24}H_{20}N_4O_3PbS$ ([$PbPh_2(OAc)(L^1)$]) (651.71): calcd. C 44.23, H 3.09, N 8.60, S 4.92; found C 43.75, H 3.08, N 8.85, S 5.15. ^{1}H NMR ([D_6]DMSO): δ = 11.06 [br. s, 1 H, N(4)H], 8.95, 8.87 [br. s, 2 H, N(1)H_2], 8.23 [d, 1 H, C(7)H], 7.82 [d, ^3J(^{1}H-^{207}Pb = 193 Hz, 4 H), $H_{o\text{-}Ph}$], 7.48 (t, 4 H, $H_{m\text{-}Ph}$), 7.34 (t, 2 H, $H_{p\text{-}Ph}$), 7.26 (t, 1 H, C_5 H), 7.01 [t, 1 H, C(6)H], 6.84 [d, 1 H, C(4)H] ppm.

[$PbPh_2(OAc)(L^2)$]: A methanolic solution (35 mL) of freshly prepared diphenyllead(IV) acetate (0.400 g, 0.85 mmol) was added to a hot solution of the ligand HL^2 (0.200 g, 0.85 mmol) in the same solvent. The orange solution was heated under reflux for 3 h and allowed to cool. The solution was filtered to remove a slight cloudiness. The clear solution was then concentrated to half its initial volume until an orange solid formed. This solid was filtered off and vacuum dried; yield 30%, m.p. 228 °C (dec.). $C_{24}H_{22}N_4O_3PbS$ {[$PbPh_2(OAc)(L^2)$]} (653.72): calcd. C 44.10, H 3.39, N 8.57, S 4.90; found C 43.63, H 3.55, N 8.54, S 4.06. ^{1}H NMR ([D_6]-DMSO): δ = 11.02 [br. s, 1 H, N(4)H], *9.61*, 9.19, *9.3* [br. s, 1 H, N(1)H], *8.23*, 8.03, *7.68* [d, 1 H, C(7)H], 7.83, *7.81* [d, ^3J(^{1}H-^{207}Pb) ≈ 198 Hz, 4 H, $H_{o\text{-}Ph}$], *7.52*, 7.48 (t, 4 H, $H_{m\text{-}Ph}$), 7.36, *7.33* (t, 2 H, $H_{p\text{-}Ph}$), *7.28*, 7.24 [t, 1 H, C(5)H], 7.06, *7.02* [t, 1 H, C(6)H], 6.86, *6.82* [d, 1 H, C(4)H], *3.20*, 3.11, *3.05* [s, 3 H, C(10)H_3], 1.72 (s, 3 H, CH_3, OAc) ppm. ^{13}C NMR ([D_6]DMSO): δ = *185.2*, 178.9 (C1), 178.7 (COO), *167.2*, 166.7 (C3), *166.6*, 166.4 [^1J(^{13}C-Pb^{207}) = 1574 Hz, $Ci_{\text{-}Ph}$], 141.5, *140.4* (C9), *136.7*, 135.2 (C2), 132.7, *132.5* [^2J (^{13}C-Pb^{207}) = 119.7 Hz, $C_{o\text{-}Ph}$], 131.1 (C5), *130.1*, 130.0 [^3J(^{13}C-Pb^{207}) = 194 Hz, $C_{m\text{-}Ph}$], 129.4 ($C_{p\text{-}Ph}$), 126.4, *125.6*, *119.9* (C7), 122.8, *122.3* (C6), *117.3*, 116.9 (C8), 111, *110.8* (C4), *31.8*, 31.0 (C10), 23.2 ($CH_{3\cdot OAc}$) ppm. One week later, a small amount of

[$PbPh_2(OAc)(N^3$-$L^2)]\cdot H_2O$ monocrystals, suitable for X-ray diffraction, were isolated from the mother liquor.

[Pb(OAc)(L^1)]: A solution of lead(II) acetate trihydrate (0.340 g, 0.91 mmol) in methanol (20 mL) was slowly added to a solution of HL^1 (0.200 g, 0.91 mmol) in the same solvent (20 mL). An orange solid formed immediately and the mixture was stirred and heated under reflux for 3 h. The mixture was cooled to r.t. and the solid was removed by filtration and dried under vacuum; yield 40%, m.p. 237 °C (dec.). $C_{11}H_{10}N_4O_3PbS$ {[Pb(OAc)(L^1)]} (485.49): calcd. C 27.21, H 2.08, N 11.54, S 6.60; found C 27.28, H 1.94, N 11.32, S 6.56. ^{1}H NMR ([D_6]DMSO): δ = 11.05 [br. s, 1 H, N(4)H], *8.36*, 7.73 [d, 1 H, C(7)H], 8.30 [br. s, 2 H, N(1)H_2], *7.26*, 7.24 [t, 1 H, C(5)H], *7.02*, 7.01 [t, 1 H, C(6)H], *6.91*, 6.88 [d, 1 H, C(4)H], 1.63 (s, 3 H, CH_3, OAc) ppm. ^{13}C NMR ([D_6]DMSO): δ = *187.1*, 183.0 (C1), 177.5 (COO), *168.2*, 158.6 (C3), *140.9*, 140.3 (C9), *137.2*, 136.1 (C2), *129.9*, 129.0 (C5), *126.4*, 119.9 (C7), 122.8, *118.2* (C8),121.9 (C6), 110.3 (C4), 26.6 (CH_3, OAc) ppm.

A crystalline solid formed on the slow evaporation of the mother liquor. Examination of this solid by stereoscopic microscopy showed a mixture of two types of crystals, mainly yellow prisms and a few orange octahedrons, both of which were suitable for X-ray analyses and had the compositions: **[Pb(OAc)(N^2-L^1)]** and **[Pb(OAc)(N^3-L^1)]·3H_2O**, respectively. A small sample of the yellow crystals (**[Pb(OAc)(N^2-L^1)]**) was selected by hand and characterized by ^{1}H and ^{13}C NMR spectroscopy in [D_6]DMSO and ^{1}H NMR spectroscopy in [D_4]MeOH. The evolution of the complex in both solvents was followed by ^{1}H NMR spectroscopy and spectra of the sample recorded at different time intervals. The results (see also Figure 10) are as follows: **(a) *t* = 0**. ^{1}H NMR ([D_6]DMSO): δ = 11.03 [br. s, 1 H, N(4)H], 8.30 [br. s, 2 H, N(1)H_2], 7.73 [d, 1 H, C(7)H], 7.23 [t, 1 H, C(5)H], 7.00 [t, 1 H, C(6)H], 6.87 [d, 1 H, C(4)H], 1.63 (s, 3 H, CH_3, OAc) ppm. ^{13}C NMR ([D_6]DMSO): δ = 183.1 (C1), 177.4 (COO), 158.6 (C3), 140.3 (C9), 136.2 (C2), 129.0 (C5), 122.9 (C8), 121.9 (C6), 119.9 (C7), 110.3 (C4), 26.6 (CH_3, OAc) ppm. ^{1}H NMR ([D_4]MeOH): δ = 7.70 [d, 1 H, C(7)H], 7.30 [t, 1 H, C(5)H], 7.06 [t, 1 H, C(6)H], 6.91 [d, 1 H, C(4)H], 1.87 (s, 3 H, CH_3, OAc) ppm. **(b) *t* = 1 week**. ^{1}H NMR ([D_6]-DMSO): δ = 10.90 [br. s, 1 H, N(4)H], 8.55, *8.30*, 8.20 [br. s, 2 H, N(1)H_2], 8.36, *7.73* [d, 1 H,C(7)H], 7.23 [t, 1 H, C(5)H], 7.00 [t, 1 H, C(6)H], 6.87 [d, 1 H, C(4)H], 1.63 (s, 3 H, CH_3, OAc) ppm. Similar spectra (in terms of signal positions and integrations) were obtained two weeks and one month later. ^{1}H NMR ([D_4]MeOH): δ = *8.40*, 7.71 [d, 1 H, C(7)H], *7.32*, 7.30 [t, 1 H, C(5)H], *7.09*, 7.06 [t, 1 H, C(6)H], *6.95*, 6.91 [d, 1 H, C(4)H], 1.87 (s, 3 H, CH_3, OAc) ppm.

[Pb(OAc)(L^2)]: A solution of lead(II) acetate trihydrate (0.160 g, 0.43 mmol) in methanol (10 mL) was slowly added to a solution of HL^2 (0.100 g, 0.43 mmol) in the same solvent (25 mL). After a few minutes, an orange solid precipitated from the yellow solution and the resulting suspension was heated under reflux for 3 h. The mixture was cooled to r.t. and the solid was removed by filtration and dried under vacuum; yield 38%, m.p. 232 °C (dec.). $C_{12}H_{12}N_4O_3PbS$ ([Pb(OAc)(L^2)]) (499.51): calcd. C 28.80, H 2.42, N 11.20, S 6.39; found C 29.12, H 2.36, N 11.11, S 6.80. ^{1}H NMR ([D_6]DMSO): δ = 10.96 [br. s, 1 H, N(4)H], *9.14*, 8.75, *8.37* [br. s, 1 H, N(1)H], *8.33*, *8.11*, 7.71 [d, 1 H, C(7)H], *7.29*, 7.22 [t, 1 H,C(5)H], *7.07*, 7.01, *7.00* [t, 1 H,C(6)H], *6.93*, *6.90*, 6.87 [d, 1 H, C(4)H], *3.04*, *2.97*, 2.95 [d, 3 H, C(10)H_3], 1.63 (s, 3 H, CH_3, OAc) ppm. ^{13}C NMR ([D_6]DMSO): δ = *190.1*, 184.3, 183.5 (C1), 177.4 (COO), *168.5*, *168.0*, 158.7 (C3), *141.4*, *140.1*, 139.8, *139.0* (C9), *135.1*, 134.7 (C2), *130.2*, *129.0*, 128.5 (C5), *126.3*, *125.6*, 119.4 (C7), 122.3, *118.3*, *117.9* (C8), *123.9*, 121.7 (C6), *110.4*, 110.3 (C4), *32.4*, 32.1, 30.5 (C10), 26.6 (CH_3, OAc) ppm.

X-ray Structure Determination: Crystal data were collected on a Bruker Smart CCD-1000 diffractometer for HL^2 and on a Bruker x8 Kappa APEX II instrument for all the complexes, at 110 K. Data were corrected for absorption by multi-scan (SADABS).[21] The data for [$PbPh_2(OAc)(N^3$-$L^2)]\cdot H_2O$ (twinned) were processed with GEMENI and SAINT.[22] Structures were solved by direct methods for the ligand and the Patterson method for the com-

Table 9. Crystal data, data collection and refinement details for the ligand and complexes.

	$HL^2\cdot H_2O$	[$PbPh_2(OAc)(N^2$-$L^1)]\cdot$ MeOH·EtOH	[$PbPh_2(OAc)(N^3$-$L^2)]\cdot H_2O$	[Pb(OAc)(N^3-L^1)]·3H_2O	[Pb(OAc)(N^2-L^1)]
Empirical formula	$C_{10}H_{12}N_4O_2S$	$C_{26}H_{30}N_4O_5PbS$	$C_{24}H_{24}N_4O_4PbS$	$C_{11}H_{16}N_4O_6PbS$	$C_{11}H_{10}N_4O_3PbS$
M	252.30	717.79	671.72	539.53	485.48
Crystal system	monoclinic	triclinic	triclinic	tetragonal	monoclinic
Space group	$P2_1/c$	$P\bar{1}$	$P\bar{1}$	$I4_1/a$	$P2_1/c$
a [Å]	8.8290(3)	11.1922(5)	10.1933(12)	15.5805(8)	8.278 (5)
b [Å]	12.9946(4)	11.6052(4)	11.4755(15)	15.5805(8)	15.412(5)
c [Å]	10.1211(3)	12.2181(6)	13.0474(18)	26.4015(12)	11.702(5)
α [°]	90	84.638(2)	95.216(8)	90	90
β [°]	93.953(2)	74.790(3)	112.206(7)	90	115.707(5)
γ [°]	90	64.979(2)	113.602(7)	90	90
V [Å^3]	1158.42(6)	1387.40(10)	1240.9(3)	6409.0(5)	1345.2(11)
Z	4	2	2	16	4
D_c [Mg m^{-3}]	1.447	1.718	1.798	2.237	2.397
μ [mm^{-1}]	0.276	6.197	6.919	10.695	12.709
F(000)	528	704	652	4096	904
Crystal size [mm]	0.53×0.45×0.21	0.23×0.18×0.07	0.27×0.12×0.06	0.25×0.14×0.07	0.05×0.04×0.03
θ range for data collection [°]	2.31–29.57	1.73–25.68	1.76–25.35	1.52–26.01	2.34–26.47
Index ranges *h*,*k*,*l*	–12, 12; 0, 18; 0, 14	–12, 13; –13, 14; 0, 14	–12, 11; –13, 13; 0, 15	–19, 19; –19, 19; –32, 32	–10, 9; 0, 19; 0, 14
Reflections collected	26295	40617	37687	20985	14244
Unique reflections, *R*	3238 [R_{int} = 0.0225]	5227 [R_{int} = 0.0461]	4527 [R_{int} = 0.1331]	3153 [R_{int} = 0.0579]	2765 [R_{int} = 0.0817]
Final R_1, wR_2 [$I>2\sigma(I)$]	0.0280, 0.0731	0.0258, 0.0523	0.0933, 0.2231	0.0410, 0.0729	0.0374, 0. 0685
(all data)	0.0307, 0.0749	0.0329, 0.0544	0.1236, 0.2561	0.0648, 0.0800	0.0553, 0.0731

plexes, followed by normal difference Fourier techniques, and refined using SHELXS-97.[23] All hydrogen atoms were introduced into calculated positions, except those of the ligand HL^2, which were located, and those of the water molecules in [Pb(OAc)-(N^3-L^1)]·$3H_2O$, which were neither located nor included in the refinement but were included in the molecular formula. Molecular graphics were obtained with ORTEP-3[24] and MERCURY.[25]

Although the crystallographic data for [$PbPh_2$(OAc)(L^2)] and for the complexes of Pb^{II} were not of high quality, successive refinements allowed the full resolution of the structures and the location of the atoms with acceptable precision. Experimental details and crystal and refinement data are listed in Table 9.

CCDC-765721 (for HL^2), 765722 {for [$PbPh_2$(OAc)(N^2-L^1)]·MeOH·EtOH}, 765723 {for [$PbPh_2$(OAc)(N^3-L^2)]·H_2O}, 765724 {for [Pb(OAc)(N^3-L^1)]·$3H_2O$} and 765725 {for [Pb(OAc)(N^2-L^1)]} contain the supplementary crystallographic data for this paper. These data can be obtained free of charge from The Cambridge Crystallographic Data Centre via www.ccdc.cam.ac.uk/data_request/cif.

Computational Details: DFT calculations were carried out to investigate the relative structural stability of [Pb(OAc)(N^2-L^1)] and [Pb(OAc)(N^3-L^1)]. Specifically, we employed the B3LYP method, which consists of a combination of Becke's three-parameter nonlocal hybrid exchange potential[26,27] and the nonlocal correlation functional of Lee, Yang and Parr.[28] The 6-31+G(d,p) basis set was used for all the atoms except Pb, for which the LanL2DZ effective core potential basis function[29] was employed. With this level of theory, the conformations of the N^2 and N^3 isomers were optimized in the gas phase using, as starting points, geometries taken from the corresponding X-ray crystallographic structures. Frequency calculations were subsequently performed to ensure that the optimized structures correspond to minima on the potential energy surface and to compute zero-point vibrational energies (ZPE). Finally, solvent effects were considered by single-point B3LYP calculations with the polarizable continuum model (PCM),[30–33] using dimethyl sulfoxide as solvent. All the calculations were performed with the Gaussian 03 package.[34]

Supporting Information (see also the footnote on the first page of this article): Figures S1 and S2 show association by hydrogen bonding forming chains in the lattice of HL^2 and [$PbPh_2$(OAc)(N^2-L^1)]·MeOH·EtOH, respectively. Figures S3 and S4 show the packing in the lattice of [$PbPh_2$(OAc)(N^2-L^1)]·MeOH·EtOH and [Pb(OAc)-(N^2-L1)], respectively. Figure S5 shows the tetrameric association by hydrogen bonding in [Pb(OAc)(N^3-L^1)]. Figure S6 represents a parallel view along the *b* axis of the [Pb(OAc)(N^3-L^1)]·$3H_2O$ lattice.

Acknowledgments

We thank the Spanish Ministry of Education and Science (MEC) (Project CTQ2006-11805) and the Spanish Ministry of Science and Innovation (MICINN) (Project CTQ2009-10738) for financial support.

[1] e. g; a) D. Kovala-Demertzi, J. R. Miller, N. Kourkoumeles, S. K. Hadjikakoi, M. A. Demertzis, *Polyhedron* **1999**, *18*, 1005–1013; b) D. J. Leggett, W. A. E. McBryde, *Talanta* **1974**, *21*, 1005–1011.
[2] J. S. Casas, E. E. Castellano, A. Macías, M. C. Rodríguez-Argüelles, A. Sánchez, J. Sordo, *J. Chem. Soc., Dalton Trans.* **1993**, 353–354.
[3] F. H. Allen, *Acta Crystrallogr., Sect. B* **2002**, *58*, 380–388.
[4] F. Basuli, S.-M. Peng, S. Bhattacharya, *Inorg. Chem.* **2000**, *39*, 1120–1127.
[5] J. S. Casas, E. E. Castellano, J. Ellena, M. S. García-Tasende, A. Sánchez, J. Sordo, A. Touceda-Varela, *Inorg. Chem. Commun.* **2004**, *7*, 1109–1112.
[6] D. Mishra, S. Naskar, M. G. B. Drew, S. K. Chattopadhyay, *Polyhedron* **2005**, *24*, 1861–1868.
[7] a) S. N. Pandeya, S. Smitha, M. Jyoti, S. K. Sridhar, *Acta Pharm.* **2005**, *55*, 27–46; b) M. D. Hall, N. K. Salam, J. L. Hellawell, H. M. Fales, C. B. Kensler, J. A. Ludwig, G. Szkács, D. E. Hibbs, M. M. Gottesman, *J. Med. Chem.* **2009**, *52*, 3191–3204.
[8] a) V. E. Ivanov, N. G. Tikhomirova, A. B. Tomchin, N. V. Razukrantova, *Pharm. Chem. J.* **1989**, *23*, 413–415; b) J. C. Logan, M. P. Fox, J. H. Morgan, A. M. Makohon, C. J. Pfau, *J. Gen. Virol.* **1975**, *28*, 271–283.
[9] H. Stünzi, *Aust. J. Chem.* **1982**, *35*, 1145–1155.
[10] M. C. Rodríguez-Argüelles, A. Sánchez, M. Belicchi Ferrari, G. Gasparri Fava, C. Pelizzi, G. Pelosi, R. Albertini, P. Lunghi, S. Pinelli, *J. Inorg. Biochem.* **1999**, *73*, 7–15.
[11] E. Labisbal, A. Sousa, A. Castiñeiras, J. A. García-Vázquez, J. Romero, D. X. West, *Polyhedron* **2000**, *19*, 1255–1262.
[12] J. S. Casas, A. Castiñeiras, M. C. Rodríguez-Argüelles, A. Sánchez, J. Sordo, A. Vázquez-López, E. M. Vázquez-López, *J. Chem. Soc., Dalton Trans.* **2000**, 4056–4063.
[13] J. S. Casas, J. Sordo, M. J. Vidarte, in: *Lead, Chemical, Analytical Aspects, Environmental Impact and Health Effects* (Eds.: J. S. Casas, J. Sordo), Elsevier, Amsterdam **2006**, p. 41.
[14] H. Stünzi, *Aust. J. Chem.* **1981**, *34*, 373–381.
[15] N. W. S. V. Nuwan de Silva, T. V. Albu, *Cent. Eur. J. Chem.* **2007**, *5*, 396–419.
[16] L. Simoni-Livny, J. P. Glusker, C. W. Bock, *Inorg. Chem.* **1998**, *37*, 1853–1867.
[17] a) M. C. Das, S. B. Maity, P. K. Bharadwaj, *Curr. Opin. Solid State Mater. Sci.* **2009**, *13*, 76–90, and references cited therein; b) R. García-Zarracino, H. Höpfl, M. Güizado-Rodríguez, *Cryst. Growth Des.* **2009**, *9*, 1651–1654; c) C.-Y. Guo, Y.-Y. Wang, K.-Z. Xu, H.-L. Zhu, P. Liu, Q.-Z. Shi, S.-M. Peng, *Polyhedron* **2008**, *27*, 3529–3536; d) F. Dai, H. He, D. Sun, *J. Am. Chem. Soc.* **2008**, *130*, 14064–14065; e) C. H. Ge, X. D. Zhang, Y. C. Ma, L. Guan, C. Y. Shi, X. Y. Zhang, Y. N. Guo, Q. T. Liu, *Chin. Chem. Lett.* **2007**, *18*, 1389–1391; f) Q.-Y. Liu, L. Xu, *CrystEngComm* **2005**, *7*, 87–89; g) B.-Q. Ma, H.-L. Sun, S. Gao, *Angew. Chem. Int. Ed.* **2004**, *43*, 1374–1376; h) , A. B. Ilyukhin, V. A. Ketsko, V. Yu. Kotov, A. K. Lyashchenko, *J. Struct. Chem.* **2002**, *43*, 977–979; i) A. Castiñeiras, S. Dehnen, A. Fuchs, I. García-Santos, P. Sevillano, *Dalton Trans.* **2009**, 2731–2739.
[18] U. Bergmann, A. Di Cicco, P. Wernet, E. Principi, P. Glatzel, A. Nilsson, *J. Chem. Phys.* **2007**, *127*, 174504/1–174504/5.
[19] A. Lenz, L. Ojamäe, *Chem. Phys. Lett.* **2006**, *418*, 361–367.
[20] G. J. Palenik, D. F. Rendle, W. S. Carter, *Acta Crystallogr., Sect. B* **1974**, *30*, 2390–2395.
[21] *SADABS*, Bruker AXS Inc., Madison, Wisconsin, USA, **2001**.
[22] *SMART* and *SAINT*, *Area Detector Control Integration Software*, Bruker Analytical X-ray Instruments, Inc., Madison, Wisconsin, USA, **1999**.
[23] G. M. Sheldrick, *SHELX-97*, *An Integrated System for Solving and Refining Crystal Structures from Diffraction Data*, University of Göttingen, Göttingen, Germany, **1997**.
[24] ORTEP III for Windows: L. J. Farrugia, *J. Appl. Cryst.* **1997**, *30*, 565.
[25] *MERCURY*, New Software for Searching the Cambridge Structural Database and Visualising Crystal Structures: I. J. Bruno, J. C. Cole, P. R. Edgington, M. K. Kessler, C. F. Macrae, P. McCabe, J. Pearson, R. Taylor, *Acta Crystallogr., Sect. B* **2002**, *58*, 389–397.
[26] A. D. Becke, *J. Chem. Phys.* **1993**, *98*, 5648–5652.
[27] A. D. Becke, *J. Chem. Phys.* **1992**, *96*, 2155–2160.
[28] C. Lee, W. Yang, R. G. Parr, *Phys. Rev. B* **1988**, *37*, 785–789.

[29] W. R. Wadt, P. J. Hay, *J. Chem. Phys.* **1985**, *82*, 284–298.
[30] E. Cances, B. Mennucci, J. Tomasi, *J. Chem. Phys.* **1997**, *107*, 3032–3041.
[31] B. Mennucci, J. Tomasi, *J. Chem. Phys.* **1997**, *106*, 5151–5158.
[32] M. Cossi, V. Barone, B. Mennucci, J. Tomasi, *Chem. Phys. Lett.* **1998**, *286*, 253–260.
[33] M. Cossi, G. Scalmani, N. Rega, V. Barone, *J. Chem. Phys.* **2002**, *117*, 43–54.
[34] M. J. Frisch, G. W. Trucks, H. B. Schlegel, G. E. Scuseria, M. A. Robb, J. R. Cheeseman, J. A. Montgomery, Jr., T. Vreven, K. N. Kudin, J. C. Burant, J. M. Millam, S. S. Iyengar, J. Tomasi, V. Barone, B. Mennucci, M. Cossi, G. Scalmani, N. Rega, G. A. Petersson, H. Nakatsuji, M. Hada, M. Ehara, K. Toyota, R. Fukuda, J. Hasegawa, M. Ishida, T. Nakajima, Y. Honda, O. Kitao, H. Nakai, M. Klene, X. Li, J. E. Knox, H. P. Hratchian, J. B. Cross, C. Adamo, J. Jaramillo, R. Gomperts, R. E. Stratmann, O. Yazyev, A. J. Austin, R. Cammi, C. Pomelli, J. W. Ochterski, P. Y. Ayala, K. Morokuma, G. A. Voth, P. Salvador, J. J. Dannenberg, V. G. Zakrzewski, S. Dapprich, A. D. Daniels, M. C. Strain, O. Farkas, D. K. Malick, A. D. Rabuck, K. Raghavachari, J. B. Foresman, J. V. Ortiz, Q. Cui, A. G. Baboul, S. Clifford, J. Cioslowski, B. B. Stefanov, G. Liu, A. Liashenko, P. Piskorz, I. Komaromi, R. L. Martin, D. J. Fox, T. Keith, M. A. Al-Laham, C. Y. Peng, A. Nanayakkara, M. Challacombe, P. M. W. Gill, B. Johnson, W. Chen, M. W. Wong, C. Gonzalez, J. A. Pople, *Gaussian 03*, rev. A.1, Gaussian, Inc., Pittsburgh, PA, USA, **2003**.

Received: June 18, 2010
Published Online: September 22, 2010

